A Regulatory Cascade Involving Class II ETHYLENE RESPONSE FACTOR Transcriptional Repressors Operates in the Progression of Leaf Senescence[1][C][W][OA]

Tomotsugu Koyama[2]*, Haruka Nii, Nobutaka Mitsuda, Masaru Ohta[3], Sakihito Kitajima, Masaru Ohme-Takagi, and Fumihiko Sato

Graduate School of Biostudies, Kyoto University, Sakyo, Kyoto 606–8502, Japan (T.K., H.N., F.S.); Department of Applied Biology, Kyoto Institute of Technology, Sakyo, Kyoto 606–8585, Japan (H.N., S.K.); Bioproduction Research Institute, National Institute of Advanced Industrial Science and Technology, Tsukuba, Ibaraki 305–8562, Japan (N.M., M.O., M.O.-T.); and Institute for Environmental Science and Technology, Saitama University, Sakura, Saitama 338–8570, Japan (M.O.-T.)

Leaf senescence is the final process of leaf development that involves the mobilization of nutrients from old leaves to newly growing tissues. Despite the identification of several transcription factors involved in the regulation of this process, the mechanisms underlying the progression of leaf senescence are largely unknown. Herein, we describe the proteasome-mediated regulation of class II ETHYLENE RESPONSE FACTOR (ERF) transcriptional repressors and involvement of these factors in the progression of leaf senescence in Arabidopsis (*Arabidopsis thaliana*). Based on previous results showing that the tobacco (*Nicotiana tabacum*) ERF3 (NtERF3) specifically interacts with a ubiquitin-conjugating enzyme, we examined the stability of NtERF3 in vitro and confirmed its rapid degradation by plant protein extracts. Furthermore, NtERF3 accumulated in plants treated with a proteasome inhibitor. The Arabidopsis class II ERFs AtERF4 and AtERF8 were also regulated by the proteasome and increased with plant aging. Transgenic Arabidopsis plants with enhanced expression of *NtERF3*, *AtERF4*, or *AtERF8* showed precocious leaf senescence. Our gene expression and chromatin immunoprecipitation analyses suggest that AtERF4 and AtERF8 targeted the *EPITHIOSPECIFIER PROTEIN/EPITHIOSPECIFYING SENESCENCE REGULATOR* gene and regulated the expression of many genes involved in the progression of leaf senescence. By contrast, an *aterf4 aterf8* double mutant exhibited delayed leaf senescence. Our results provide insight into the important role of class II ERFs in the progression of leaf senescence.

Leaf senescence, which is characterized by progressive yellowing, is the final stage of leaf development and involves the mobilization of nutrients from old leaves to newly growing tissues. The progression of leaf senescence requires programmed cell death combined with the cessation of photosynthesis, organelle breakdown, and protein degradation. The regulation of leaf senescence depends largely on the developmental age of plants, although it is also influenced by various external stimuli (Gan and Amasino, 1997). The detection of internal and external signals activates various processes mediated by signaling molecules such as plant hormones and reactive oxygen species (ROS; Buchanan-Wollaston et al., 2003; Lim et al., 2007).

The progression of leaf senescence is associated with the down-regulation of genes involved in chlorophyll biosynthesis, carbon metabolism, and photosynthesis and the up-regulation of genes involved in responses to hormones, ROS, and various stresses (Gepstein, 2004; Lin and Wu, 2004; Buchanan-Wollaston et al., 2005; van der Graaff et al., 2006; Balazadeh et al., 2008; Breeze et al., 2011). The coordinated regulation of gene expression during leaf senescence depends on the combined action of several families of transcription factors (TFs). In particular, genes coding for NO APICAL MERISTEM/ARABIDOPSIS TRANSLATION ACTIVATION FACTOR/CUP-SHAPED COTYLEDON (NAC), zinc finger, WRKY, MYB, and APETALA2/ETHYLENE RESPONSE FACTOR (AP2/ERF) TFs are transcriptionally up-regulated during leaf senescence (Lin and Wu, 2004; Buchanan-Wollaston et al., 2005; Breeze et al., 2011). Functional analyses using Arabidopsis (*Arabidopsis thaliana*) have revealed that NAC and WRKY TFs, including NAC-like ACTIVATED BY AP3/PI, ANAC092/ORESARA1 (ORE1), ORE1-SISTER1,

[1] This work was supported by a Grant-in-Aid for Young Scientists (B; grant no. 23770042 to T.K.).

[2] Present address: Suntory Foundation for Life Sciences, Bioorganic Research Institute, Wakayamadai, Shimamoto, Osaka 618–8503, Japan.

[3] Present address: Genetically Modified Organism Research Center, National Agriculture and Food Research Organization, Tsukuba, Ibaraki 305–8666, Japan.

* Corresponding author; e-mail koyama@sunbor.or.jp.

The author responsible for distribution of materials integral to the findings presented in this article in accordance with the policy described in the Instructions for Authors (www.plantphysiol.org) is: Tomotsugu Koyama (koyama@sunbor.or.jp).

[C] Some figures in this article are displayed in color online but in black and white in the print edition.

[W] The online version of this article contains Web-only data.

[OA] Open Access articles can be viewed online without a subscription.

www.plantphysiol.org/cgi/doi/10.1104/pp.113.218115

VND-INTERACTING2, NAC WITH TRANSMEMBRANE MOTIF-LIKE4, JUNGBRUNNEN1, WRKY6, WRKY53, WRKY54, and WRKY75, regulate leaf senescence (Robatzek and Somssich, 2002; Miao et al., 2004; Guo and Gan, 2006; Kim et al., 2009; Balazadeh et al., 2011; Besseau et al., 2012; Lee et al., 2012; Wu et al., 2012). By contrast, the role of AP2/ERF TFs in leaf senescence remains unclear.

AP2/ERF TFs consist of 146 members in Arabidopsis and are involved in responses to various external and internal stimuli. Several AP2/ERFs modulate responses to leaf senescence-associated signaling molecules such as ROS, ethylene, jasmonic acid (JA), abscisic acid (ABA), and cytokinin (Nakano et al., 2006; Mizoi et al., 2012). Gain-of-function studies suggest that RELATED TO ABI3/VP1 and C-REPEAT BINDING FACTOR/DEHYDRATION RESPONSIBLE ELEMENT BINDING1 positively and negatively regulate leaf senescence, respectively (Sharabi-Schwager et al., 2010; Woo et al., 2010). However, knowledge of the molecular mechanisms of these AP2/ERFs in the regulation of leaf senescence is lacking.

Class II ERFs are characterized by the ERF-associated amphiphilic repression (EAR) motif (Ohta et al., 2001). Because class II ERFs repress target gene transcription in the presence of ERF activators in transient gene expression assays (Fujimoto et al., 2000; Ohta et al., 2000, 2001), understanding the regulation of class II ERFs is key to elucidating the complex mechanisms underlying AP2/ERF-mediated gene regulation. In addition to studying the stress response-associated transcriptional control of class II *ERF* genes, (Suzuki et al., 1998; Yamamoto et al., 1999; Fujimoto et al., 2000; Kitajima et al., 2000; Nishiuchi et al., 2004), we previously analyzed the posttranslational regulation of class II ERFs and showed that a class II ERF from tobacco (*Nicotiana tabacum*), NtERF3, physically interacts with the ubiquitin-conjugating (UBC) enzyme NtUBC2 (Koyama et al., 2003). Coexpression of the dominant-negative form of *NtUBC2* enhances the repressive activity of NtERF3 in transient assays, suggesting that NtUBC2 may regulate NtERF3 activity. By contrast, NtUBC2 does not interact with NtERF2, a transcriptional activator. The function of NtUBC2 in the ubiquitin-proteasome system (Dreher and Callis, 2007; Vierstra, 2009) suggests that NtERF3 may be regulated by proteolysis.

In this study, we demonstrate the involvement of proteasomes in the control of NtERF3 and two homologous Arabidopsis class II ERFs, AtERF4 and AtERF8. We also performed functional and gene expression analyses to clarify the role of these class II ERFs in the progression of leaf senescence.

RESULTS

Rapid Degradation of NtERF3 in Vitro

Because NtERF3 physically and functionally interacts with NtUBC2 (Koyama et al., 2003), we first examined the regulation of NtERF3 by proteolysis in vitro (Fig. 1). NtERF3, NtERF2, and GFP, as a stable protein model, were individually produced in *Escherichia coli* and purified with affinity resin (Supplemental Fig. S1). Each protein was incubated for 0, 15, 30, and 60 min in a cultured tobacco XD6S cell extract, and protein stability was analyzed with immunoblotting. Whereas NtERF3 was extremely unstable in the tobacco cell extract solution (Fig. 1A), NtERF2 and GFP were stable for 60 min (Fig. 1, B and C). NtERF3 levels remained stable in a bovine serum albumin solution (Fig. 1D), suggesting that NtERF3 is specifically degraded by plant proteins.

To identify the amino acid residues involved in the stability of NtERF3, we produced truncated NtERF3 proteins in *E. coli* (Fig. 1E; Supplemental Fig. S1). NtERF3 contains a conserved DNA-binding domain, an EAR domain, and an NtUBC2-interacting region consisting of amino acid residues 83 to 190 (NtERF3 [83/190]; Fig. 1E; Koyama et al., 2003). Incubating NtERF3 (1/225), NtERF3 (1/190), NtERF3 (26/225), NtERF3 (83/190), and NtERF3 (83/225) in the tobacco cell extract solution caused their rapid degradation, whereas NtERF3 (Δ83/190), in which amino acid residues 83 to 190 were deleted, was degraded at a much slower rate. By contrast, NtERF3 (1/82) and NtERF3 (191/225) remained undegraded. These results suggested that NtERF3 (83/190) was essential and sufficient for NtERF3 degradation, whereas the repression and ERF domains were not involved in the stabilization of the protein. NtERF3 amino acid residues 83 to 95 contain a PEST motif, which is involved in the instability of proteins (Asher et al., 2006); however, deletion of the PEST motif did not affect the stability of NtERF3 in vitro (Fig. 1E).

Low Accumulation of NtERF3 in Plant Cells

To examine the stability of NtERF3 in plants, we individually fused the coding sequences (CDSs) for the respective regions of *NtERF3* with the nuclear localization signal (NLS)-GFP sequence under the control of the *Cauliflower mosaic virus* 35S promoter (*Pro-35S*:*NLS-GFP*), and the resulting fusion genes were transformed into cultured tobacco XD6S cells (Supplemental Fig. S2A). More than 100 kanamycin-resistant tobacco calluses for each construct were examined for GFP florescence. We detected no GFP signal in the *Pro-35S*:*NLS-GFP-NtERF3* and *Pro-35S*:*NLS-GFP-NtERF3* (*83/190*) tobacco calluses, whereas the *Pro-35S*:*NLS-GFP-NtERF3* (*1/82*) and *Pro-35S*:*NLS-GFP-NtERF3* (*191/225*) tobacco calluses showed strong nuclear GFP fluorescence (Fig. 2A). Consistent with these results, immunoblot analysis of protein extracts from *Pro-35S*:*NLS-GFP-NtERF3* (*1/82*) and *Pro-35S*:*NLS-GFP-NtERF3* (*191/225*) tobacco calluses showed positive reactivity against an anti-GFP antibody, whereas extracts from *Pro-35S*:*NLS-GFP-NtERF3* and *Pro-35S*:*NLS-GFP-NtERF3* (*83/190*) tobacco calluses were negative (Fig. 2B).

No kanamycin-resistant *Pro-35S*:*NLS-GFP-NtERF3* (*Δ83/190*) tobacco calluses were recovered, suggesting that the fusion gene may confer a lethal phenotype on tobacco cells and this lethal gene may have a less

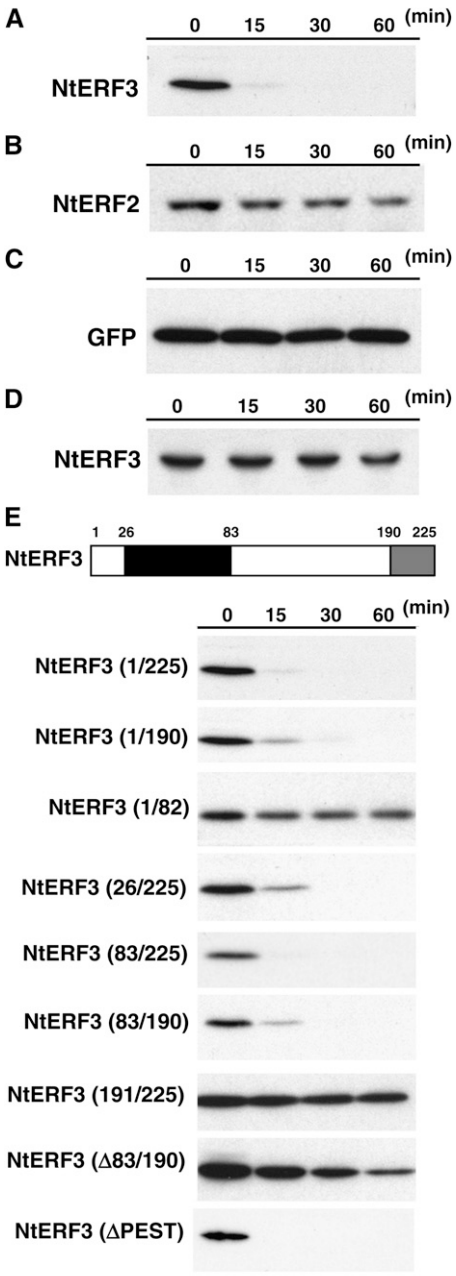

Figure 1. Rapid degradation of NtERF3 in vitro. A to D, Levels of recombinant NtERF3 (A and D), NtERF2 (B), and GFP (C) incubated in the cell extract (A–C) or bovine serum albumin (D) solutions for the indicated times. Recombinant NtERF3, NtERF2, and GFP were detected via immunoblotting using anti-NtERF3 (A and D), anti-NtERF2 (B), and anti-GFP (C) antibodies, respectively. E, Mapping the domain responsible for NtERF3 instability in vitro. The top section shows a schematic representation of NtERF3. Black and gray boxes indicate the DBD and EAR repression domain, respectively. Numbers show the position of amino acid residues from the first Met. The bottom sections show the levels of the respective regions of NtERF3 at the time points indicated in the cell extract solution. These regions of NtERF3 were detected via immunoblotting using an anti-NtERF3 antibody. The molecular size of each protein is provided in Supplemental Fig. S1.

severe effect in a heterologous system. As expected, two lines of *Pro-35S:NLS-GFP-NtERF3* (*Δ83/190*) Arabidopsis plants grew and produced small amounts of seed (Supplemental Fig. S2B; see Fig. 4). Because *Pro-35S:NLS-GFP-NtERF3* (*Δ83/190*) Arabidopsis plants exhibited a severe defective phenotype, 3-d-old seedlings were analyzed by florescence microscopy. The cells of *Pro-35S:NLS-GFP-NtERF3* (*Δ83/190*) Arabidopsis plants showed strong GFP florescence similar to that of *Pro-35S:NLS-GFP* Arabidopsis plants; the florescence was absent in *Pro-35S:NLS-GFP-NtERF3* Arabidopsis plants (Fig. 2C). These results suggest that NtERF3 levels were low in plant cells and that the NtERF3 (83/190) region may determine protein instability.

Proteasomal Degradation of Class II ERF Repressors

To characterize the mechanism underlying the proteolytic degradation of NtERF3, we treated *Pro-35S:NLS-GFP-NtERF3* Arabidopsis plants with MG132, a proteasome inhibitor. Fluorescence microscopy and immunoblot analyses showed that MG132 treatment enhanced the accumulation of NLS-GFP-NtERF3 (Fig. 3A).

We further investigated the role of proteasomes in the stability of the NtERF3 homologs AtERF4 and AtERF8 (Ohta et al., 2001). Hemaglutinin (HA)-tagged *AtERF4* and *AtERF8* under the control of the 35S promoter (*Pro-35S:AtERF4-HA* and *Pro-35S:AtERF8-HA*) were separately introduced into Arabidopsis plants (Supplemental Fig. S2B). These transgenic plants were grown for 3 weeks and treated with MG132. Immunoblot analysis showed that MG132 treatment increased AtERF4-HA and AtERF8-HA levels, whereas dimethyl sulfoxide (DMSO) treatment had no effect (Fig. 3, B and C). Furthermore, an upper-shifted band corresponding to AtERF4-HA suggested posttranslational modification of AtERF4 (Fig. 3C). These results provided evidence of the involvement of proteasome in the control of NtERF3, AtERF4, and AtERF8 stabilities.

Interestingly, AtERF4-HA and AtERF8-HA accumulated in aging plants in the absence of MG132 treatment (Fig. 3D). However, unlike MG132-treated plants, no shift of AtERF4-HA was detected in older plants. These results indicated that aging also stabilized AtERF4 and AtERF8.

Cell Death and Precocious Leaf Senescence Induced by Class II ERFs

Our study of the stability of ERF indicated that ectopic expression of class II ERF repressor genes induced a phenotype characterized by cell death and precocious leaf senescence (Fig. 4). We therefore attempted to characterize the functions of class II ERF repressors in Arabidopsis plants. Two *Pro-35S:NLS-GFP-NtERF3 (Δ83/190)* lines of Arabidopsis plants established through several independent transformation trials

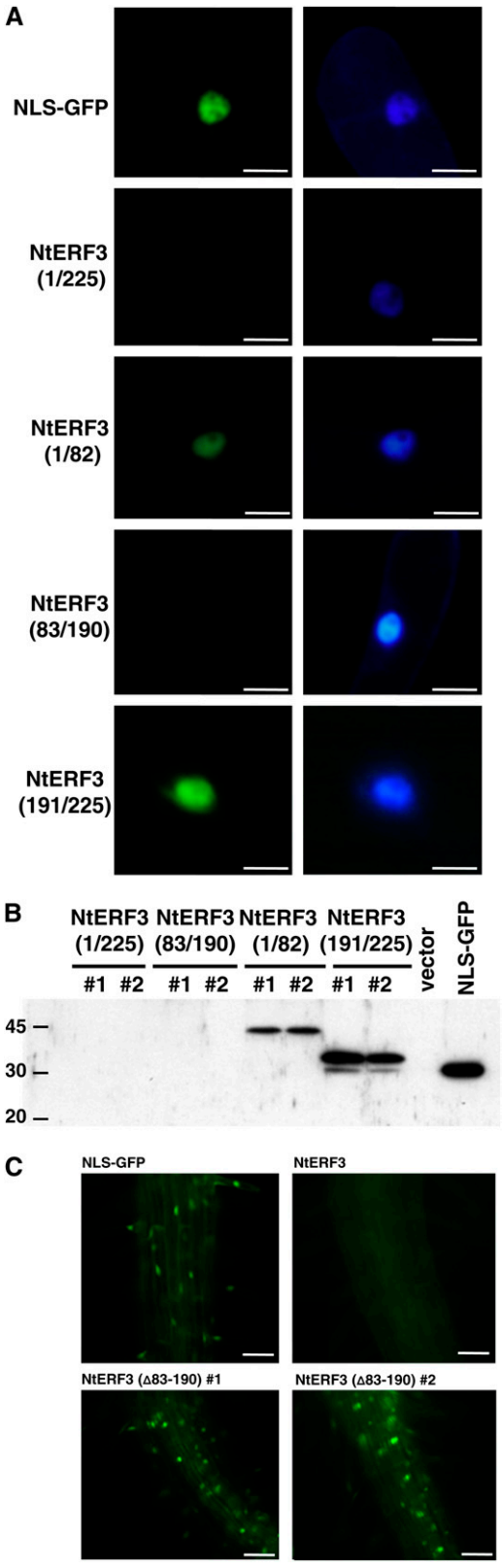

Figure 2. Low accumulation of NtERF3 in plant cells. A, GFP florescence in the nucleus of transgenic tobacco cells in which the individual fused gene was introduced (left). 4′,6-Diamidino-2-phenylindole staining (right) shows the location of the nucleus. B, Immunoblot analysis of transgenic tobacco cells after introduction of the fusion genes. Two independent lines per construct were subjected to immunoblot analysis using an anti-GFP antibody. The molecular size markers are shown on the left. C, GFP florescence of *Pro-35S:NLS-GFP-NtERF3* and *Pro-35S:NLS-GFP-NtERF3* (*Δ83/190*) roots of 3-d-old Arabidopsis seedlings. NLS, Nuclear localization signal. Bars = 10 μm (A) and 50 μm (C).

were fertile but severely deformed (Fig. 4, A and B), indicating the lethality of high NtERF3 accumulation. Transformation of *Pro-35S:NLS-GFP-NtERF3*, *Pro-35S:AtERF4-HA*, and *Pro-35S:AtERF8-HA* genes into Arabidopsis plants induced significant but relatively moderate phenotypes associated with cell death. A significant proportion of *Pro-35S:AtERF4-HA* (15 of 40 lines) and *Pro-35S:AtERF8-HA* (13 of 46 lines) Arabidopsis plants exhibited moderate phenotypes with lesions in both cotyledons and leaves, and they often died before flowering. Certain *Pro-35S:NLS-GFP-NtERF3* (two lines), *Pro-35S:AtERF4-HA* (11 lines), and *Pro-35S:AtERF8-HA* (eight lines) Arabidopsis plants exhibited mild phenotypes with smaller leaves in the seedling stage and precocious senescence in rosette leaves (Fig. 4, C–F).

The *Pro-35S:NLS-GFP-NtERF3* (*Δ83/190*), *Pro-35S:AtERF4-HA*, and *Pro-35S:AtERF8-HA* leaves with the moderate phenotypes showed strong signals of trypan blue pigment, a dead cell marker (Fig. 4G). These plants also displayed a brown precipitate owing to the reaction of hydrogen peroxide (H_2O_2) and diaminobenzidine (DAB; Fig. 4H). These results suggested that ectopic expression of *NtERF3*, *AtERF4*, and *AtERF8* caused cell death and precocious leaf senescence associated with H_2O_2 production.

Regulation of Genes Involved in Leaf Senescence by AtERF4

Because ectopic expression of the class II ERF genes examined had a similar effect on inducing cell death and precocious leaf senescence, these ERFs might regulate expression of a common set of downstream genes. Previous studies revealed the induction of *AtERF4* expression by ethylene, ABA, and JA, which regulate the progression of leaf senescence (Fujimoto et al., 2000; McGrath et al., 2005; Yang et al., 2005), and then *AtERF4* was used as a model for further characterization of downstream genes. Microarray analysis detected 929 genes transcriptionally increased more than 2-fold (P value of dependent Student's t test < 0.05; false discovery rate [FDR] < 0.04225; see "Materials and Methods") and 687 genes decreased less than one-half ($P < 0.05$) in 2-week-old *Pro-35S:AtERF4-HA* plants compared with *Pro-35S:NLS-GFP-HA* plants, which showed normal morphology. Comparative analysis of public databases revealed that a considerable number of the genes up-regulated in *Pro-35S:AtERF4-HA* plants were also up-regulated in the older

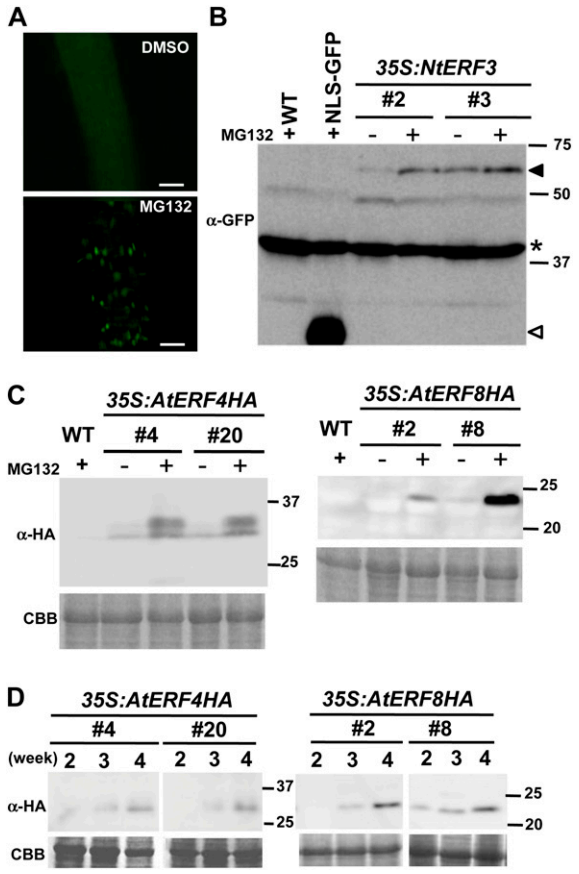

Figure 3. NtERF3, AtERF4, and AtERF8 levels in Arabidopsis plants increased by MG132 and aging. A, GFP florescence of the roots of *Pro-35S:NLS-GFP-NtERF3* Arabidopsis seedlings treated with DMSO and MG132. Bars = 50 μm. B and C, Accumulation of NLS-GFP-NtERF3 (B), AtERF4-HA, and AtERF8-HA (C) induced by MG132 treatment. Two independent lines of 3-week-old *Pro-35S:NLS-GFP-NtERF3* (*35S:NtERF3*), *Pro-35S:AtERF4-HA*, and *Pro-35S:AtERF8-HA* Arabidopsis plants treated with DMSO (–) and MG132 (+) were subjected to immunoblot analysis using anti-GFP (B) and anti-HA antibodies (C). In B, the black and white triangles indicate NLS-GFP-NtERF3 and NLS-GFP signals, respectively. Signals due to the nonspecific cross reactivity with an unknown protein (B, asterisk) and Coomassie Brilliant Blue (CBB) staining (C) serve as loading controls. Molecular size markers are shown on the right. D, Accumulation of AtERF4-HA and AtERF8-HA induced by plant aging. *Pro-35S:AtERF4-HA* and *Pro-35S:AtERF8-HA* Arabidopsis plants were grown on plates for 2, 3, and 4 weeks and subjected to immunoblot using anti-HA antibody. WT, Wild type. [See online article for color version of this figure.]

leaves of the wild type (Fig. 5). The heat map included 842 genes recorded in the data sets (Breeze et al., 2011) of the 929 genes up-regulated in *Pro-35S:AtERF4-HA* plants and showed that their transcripts increased according to the age of plants (Fig. 5). In addition, reverse transcription (RT)-PCR analysis revealed the up-regulation of senescence-associated genes *SAG12* and *SAG13* in *Pro-35S:AtERF4-HA* plants (Supplemental Fig. S3). Whereas the phenotype of *Pro-35S:AtERF4-HA* plants could be the result of senescence, hypersensitive reaction-like cell death, or other necrosis-related events (Fig. 4), our results suggested that ectopic expression of *AtERF4* induced the expression of genes associated with leaf senescence.

We searched for TF binding sites in the 1,000-bp region upstream of the transcription initiation site of the genes up-regulated in *Pro-35S:AtERF4-HA* plants

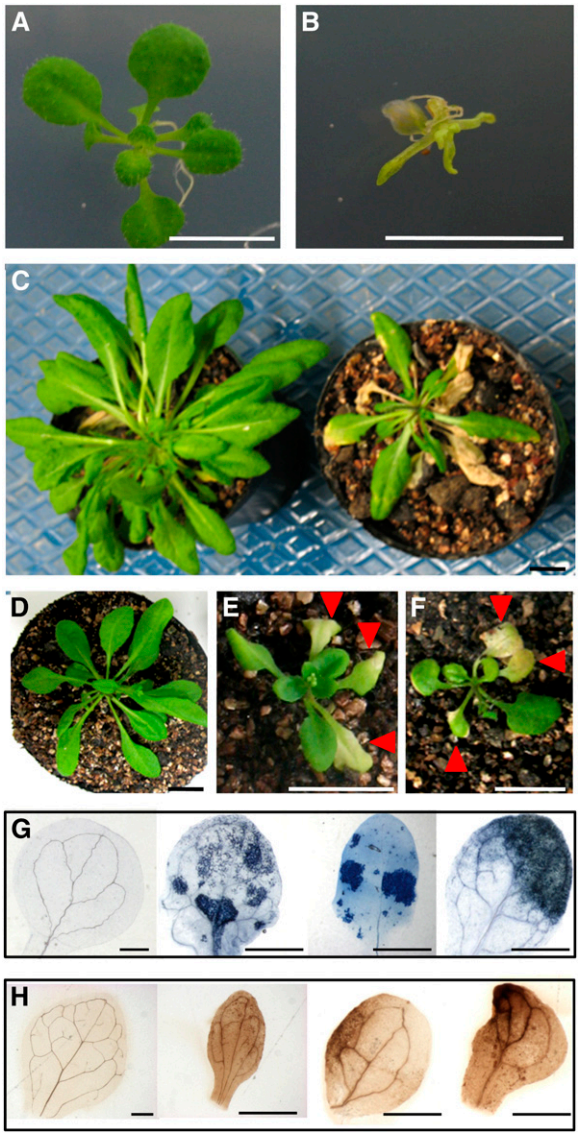

Figure 4. Ectopic expression of *NtERF3*, *AtERF4*, and *AtERF8* genes induced cell death and precocious leaf senescence. A and B, Wild-type (A) and *Pro-35S:NLS-GFP-NtERF3* (*Δ83/190*; B) Arabidopsis plants grown on Murashige and Skoog plates for 3 weeks. C, Wild-type (left) and *Pro-35S:NLS-GFP-NtERF3* (right) Arabidopsis plants grown on soil for 5 weeks. Inflorescences were detached for a detailed view. D to F, Wild-type (D), *Pro-35S:AtERF4-HA* (E), and *Pro-35S:AtERF8-HA* (F) Arabidopsis plants grown for 4 weeks. G and H, Trypan blue (G) and DAB (H) staining of wild-type, *Pro-35S:NLS-GFP-NtERF3* (*Δ83/190*), *Pro-35S:AtERF4-HA*, and *Pro-35S:AtERF8-HA* leaves of 3-week-old Arabidopsis plants (from left to right). Bars = 1 cm (A–F) and 0.5 mm (G and H).

and found that the group of genes containing a W-box, which is a binding motif of WRKY TFs, was overrepresented (Supplemental Table S1). Consistently, 17 of 71 *WRKY* genes were significantly up-regulated in *Pro-35S:AtERF4-HA* plants (Supplemental Tables S2 and S3). Among them, *WRKY30*, *WRKY53*, and *WRKY75* were positive regulators of leaf senescence, whereas *WRKY18*, *WRKY40*, and *WRKY60* were involved in the basal defense response against pathogen attack (Xu et al., 2006; Miao and Zentgraf, 2007; Besseau et al., 2012; Li et al., 2012). In our RT-PCR analysis, *WRKY18*, *WRKY30*, *WRKY40*, *WRKY53*, *WRKY60*, and *WRKY75* transcripts were increased in *Pro-35S:AtERF4-HA* and *Pro-35S:AtERF8-HA* plants (Fig. 6), indicating that AtERF4 and AtERF8 regulated the expression of these genes.

Conversely, *Pro-35S:AtERF4-HA* plants showed reduced expression of the genes down-regulated in aging plants. Our comparative analysis revealed that *AUXIN/INDOLE-3-ACETIC ACID* (*AUX/IAA*) genes, which are negative regulators of auxin responses and down-regulated in senescent leaves (van der Graaff et al., 2006), were overrepresented in the genes down-regulated in *Pro-35S:AtERF4-HA* plants (Supplemental Tables S2 and S4). Moreover, *EPITHIOSPECIFIER PROTEIN/EPITHIOSPECIFYING SENESCENCE REGULATOR*

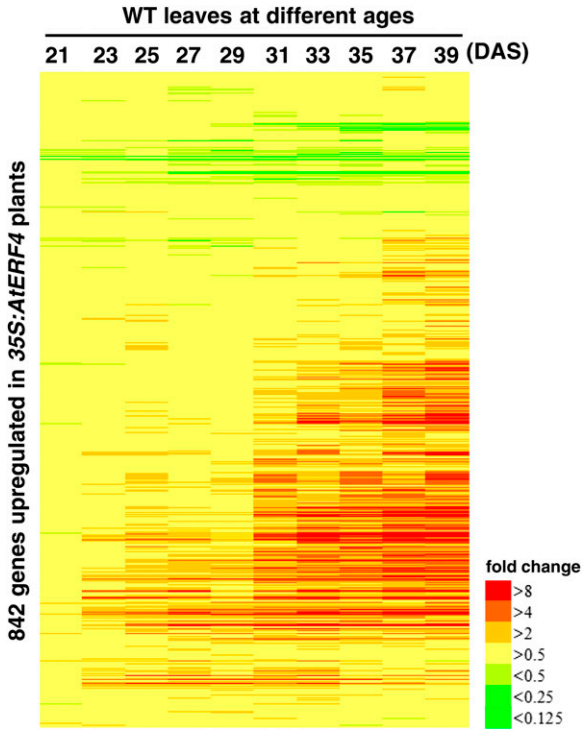

Figure 5. Expression of the genes regulated by AtERF4 in response to plant aging. Genes up-regulated by AtERF4 are aligned along the vertical axis, and the ages of wild-type (WT) Arabidopsis plants are given along the horizontal axis. The bar represents the transcript level of each gene and is colored according to the extent of fold change in the data set (Breeze et al., 2011).

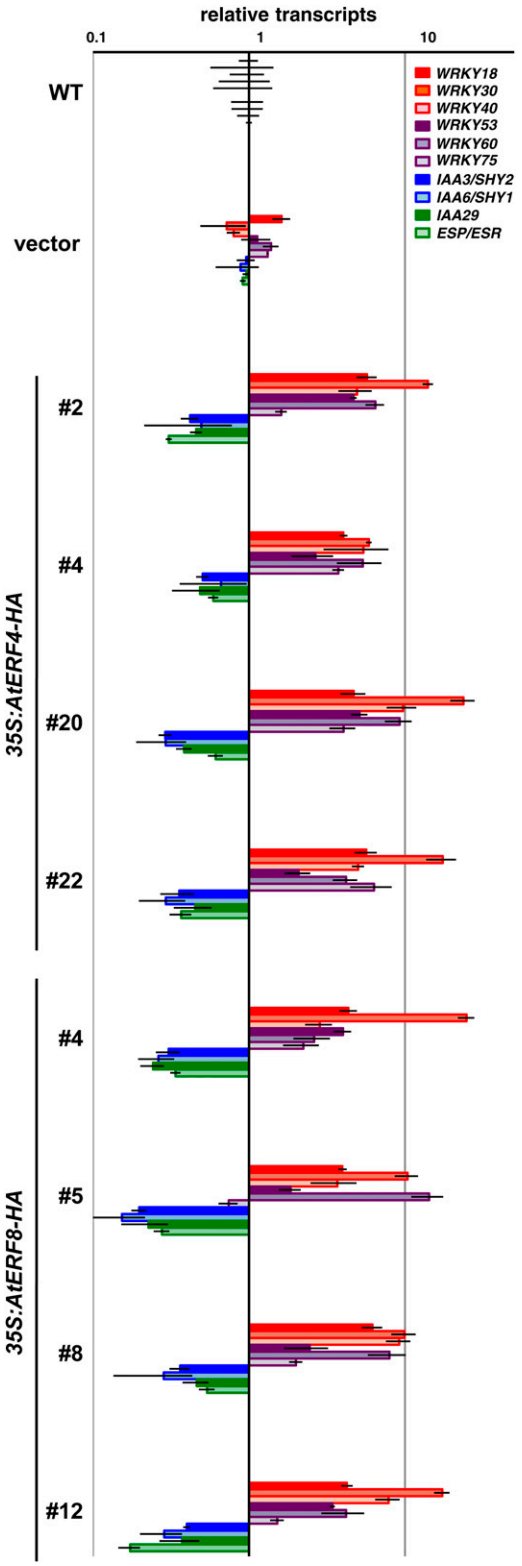

Figure 6. Expression of the genes downstream of the class II ERFs in *35S:AtERF4-HA* and *35S:AtERF8-HA* Arabidopsis plants. Transcript levels were determined with RT-PCR of aliquots of total RNAs from wild-type (WT), *Pro-35S:NLS-GFP-HA* (vector), and four independent lines of *Pro-35S:AtERF4-HA* and *Pro-35S:AtERF8-HA* Arabidopsis plants. The wild-type values were set at 1. Error bars indicate SD.

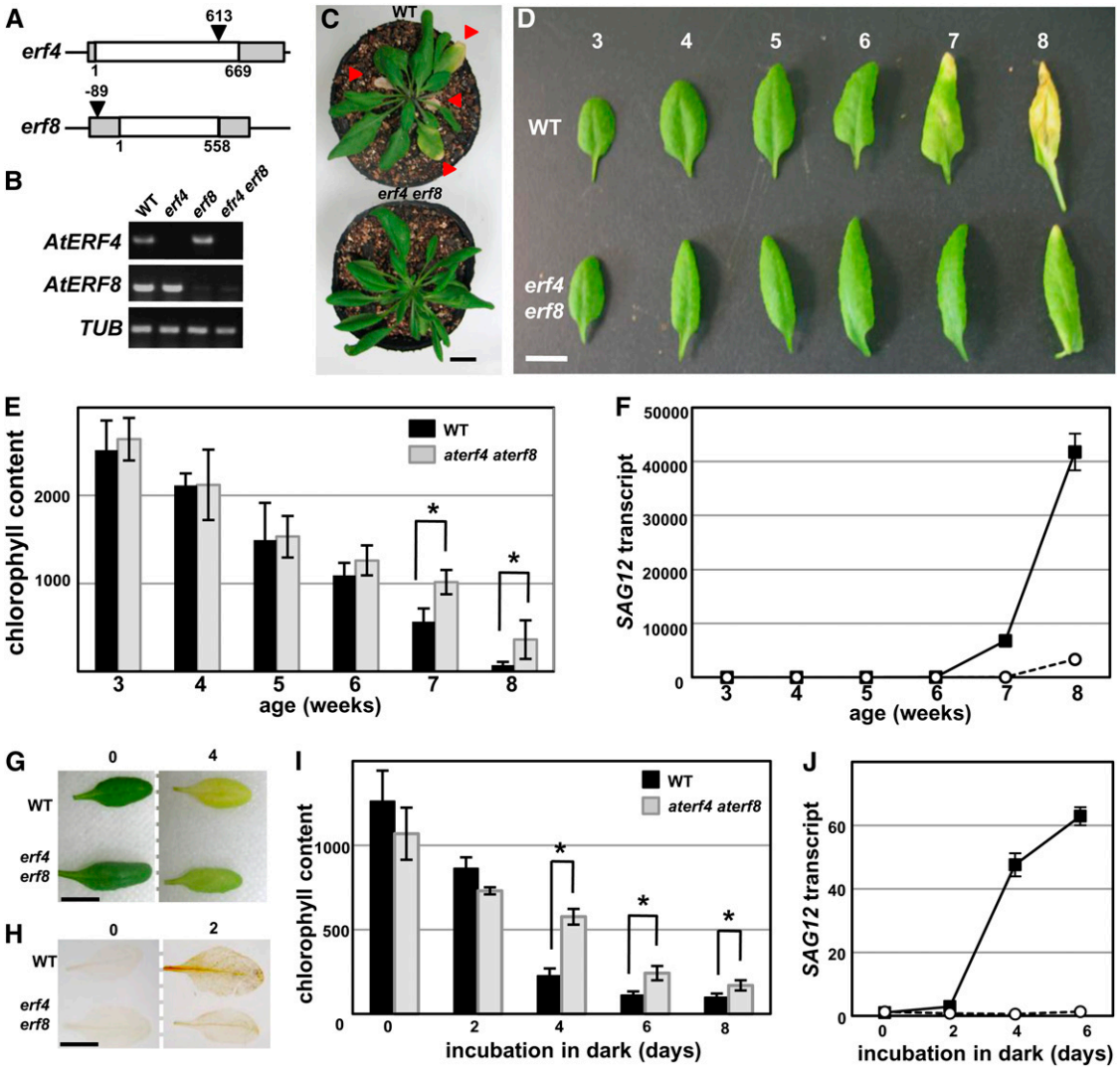

Figure 7. Delayed leaf senescence in an *aterf4 aterf8* double mutant. A, Schematic diagrams of the *AtERF4* and *AtERF8* structures and the transfer DNA tag insertions. The white and gray boxes represent coding and untranslated regions, respectively. The triangles show the transfer DNA insertion site. Numbers indicate positions of the transfer DNA tag insertion relative to the translational initiation site. B, *AtERF4* and *AtERF8* transcripts in *aterf4* and *aterf8* mutants and *aterf4 aterf8* double mutants. The CDSs of *AtERF4* and *AtERF8* were amplified by RT-PCR of aliquots of total RNAs from 3-week-old wild type (WT) and *erf* mutants. An extraordinarily low level of *AtERF8* transcript was detected in *aterf8* mutants and *aterf4 aterf8* double mutants. C, Rosettes of 6-week-old wild-type (left) and *aterf4 aterf8* (right) plants. Triangles indicate senescing leaves. Inflorescences were detached for detailed view. D, The sixth leaf of wild-type (top) and *aterf4 aterf8* (bottom) plants of different ages. E, Chlorophyll content of the sixth leaf of wild-type and *aterf4 aterf8* plants at indicated ages. The error bars and asterisks indicate SD ($n = 12$) and SDs at $P < 0.001$ by Student's *t* test. F, *SAG12* transcript was determined by RT-PCR of aliquots of total RNAs from the sixth leaves of wild-type (black squares) and *aterf4 aterf8* (white circles) plants at the indicated ages. The values of 3-week-old wild-type leaves were set at 1. Error bars indicate SD of technical triplicates. G, Dark-induced senescence in wild-type and *aterf4 aterf8* leaves. The detached leaves were photographed on days 0 (left) and 4 (right) after incubation in the dark. H, DAB staining of the detached leaves at 0 (left) and 2 (right) d after incubation in the dark. I, Chlorophyll content in wild-type and *aterf4 aterf8* leaves at indicated days after incubation in the dark. The error bars and asterisks indicate SD ($n = 7$) and SDs at $P < 0.001$ by Student's *t* test. J, The *SAG12* transcript was determined with RT-PCR using aliquots of total RNAs from wild-type (black squares) and *aterf4 aterf8* (white circles) leaves incubated for the indicated days in dark. The values of wild-type leaves at day 0 were set at 1. Error bars indicate SD of technical triplicates. Bars = 1 cm.

(*ESP/ESR*), a negative regulator of leaf senescence via the antagonistic modulation of WRKY53 activity at the transcriptional and posttranslational levels (Miao and Zentgraf, 2007), was down-regulated in *Pro-35S:AtERF4-HA* plants. RT-PCR analysis showed that transcripts for *IAA3/SHORT HYPOCOTYL2* (*SHY2*), *IAA6/SHY1*,

IAA29, and *ESP/ESR* were reduced in *Pro-35S:AtERF4-HA* and *Pro-35S:AtERF8-HA* plants (Fig. 6). The gene expression profiles of these plants were consistent with the precocious leaf senescence phenotype.

Delayed Leaf Senescence in an *aterf4 aterf8* Double Mutant

To clarify the physiological role of class II ERFs in plants, we established *aterf4* and *aterf8* single and *aterf4 aterf8* double mutants (Fig. 7, A and B). Whereas the single mutants had apparently normal leaves, the *aterf4 aterf8* double mutant had irregular, downward curled leaves and delayed leaf yellowing (Fig. 7, C and D; Supplemental Fig. S4). The age-dependent reduction of chlorophyll content and activation of senescence marker gene *SAG12* in wild-type leaves was delayed in the leaves of the *aterf4 aterf8* mutant (Fig. 7, E and F). A dark-induced senescence assay demonstrated that mature leaves of the wild type incubated in the dark displayed yellowing (Oh et al., 1997; Weaver and Amasino, 2001), whereas those of the *aterf4 aterf8* double mutants showed delayed yellowing (Fig. 7G). DAB staining demonstrated that H_2O_2 accumulated significantly in dark-induced senescing leaves of wild-type plants but to a lesser degree in the *aterf4 aterf8* mutant (Fig. 7H). The dark-induced decline of chlorophyll content was also delayed in *aterf4 aterf8* mutant leaves, and activation of *SAG12* expression was inhibited (Fig. 7, I and J). These results indicated that *aterf4 aterf8* delayed leaf senescence.

In the leaves of the *aterf4 aterf8* mutant, the expression of genes involved in the positive regulation of leaf senescence was down-regulated, whereas that of the negative regulator genes was increased (Fig. 8). *WRKY30*, *WRKY53*, and *WRKY75* transcripts were low in the mature leaves of the wild type and subsequently increased in older leaves, but were maintained at low levels in mature and old leaves of *aterf4 aterf8* mutants. Conversely, *IAA3/SHY2*, *IAA6/SHY6*, and *ESP/ESR* transcripts in mature leaves of the *aterf4 aterf8* mutant were increased compared with those of the wild type, whereas these transcripts were gradually reduced in older leaves (Fig. 8; Supplemental Fig. S5). Taken together, these results suggest that the delayed leaf senescence phenotype of the *aterf4 aterf8* mutant was responsible for changes in the expression profile.

Delayed leaf senescence in *aterf4 aterf8* plants was unlikely to have resulted from general growth retardation because flowering time in this mutant was comparable to that of wild-type plants (Supplemental Fig. S6). Furthermore, no defects in the general components of the ethylene and JA response pathways in the *aterf4 aterf8* mutant was detected; it progressed at a pace similar to that of the wild type in the presence of 1-aminocyclopropanecarboxylic acid, a precursor of ethylene, and methyl jasmonate (Supplemental Fig. S7).

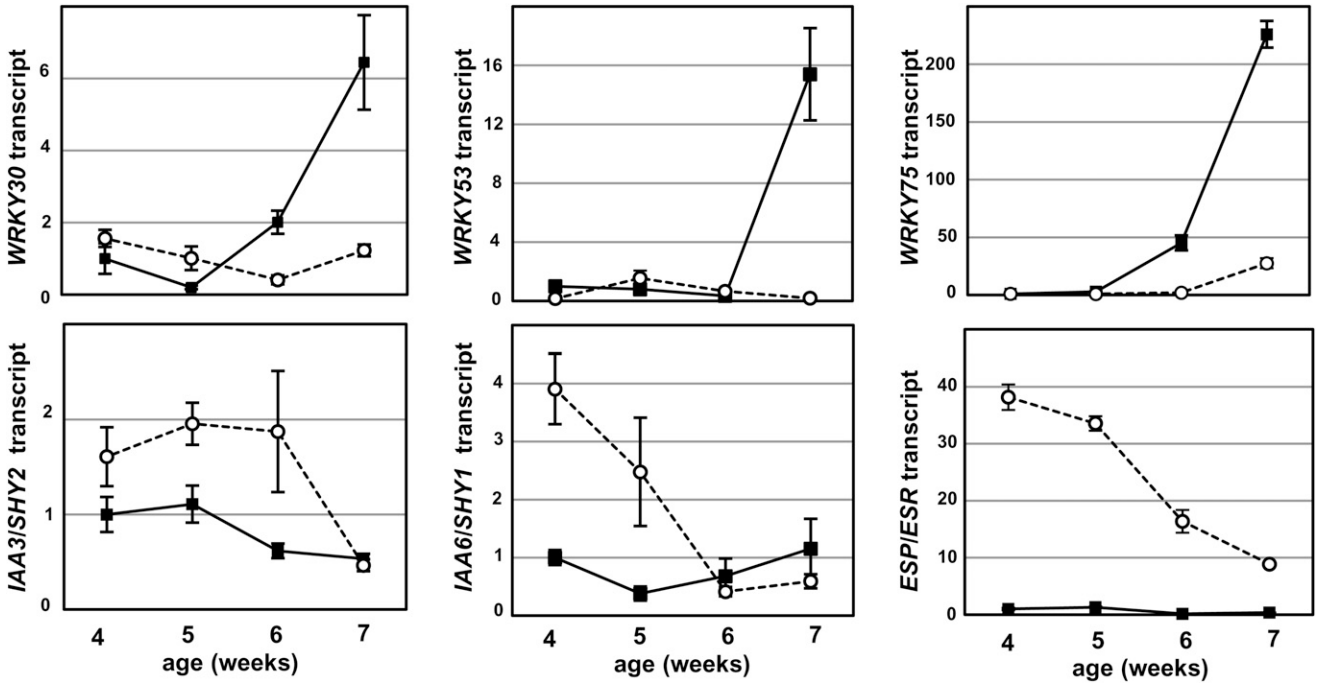

Figure 8. Expression of leaf senescence-related genes during the aging of wild-type and *aterf4 aterf8* plants. Transcript levels were determined with RT-PCR using aliquots of total RNAs from the sixth leaves of wild-type (black squares) and *aterf4 aterf8* (white circles) plants at the indicated ages. The values of 4-week-old wild-type leaves were set at 1. Error bars indicate SD of technical triplicates.

Binding of AtERF4 and AtERF8 to *ESP/ESR*

Because AtERF4 and AtERF8 function primarily as transcriptional repressors (Ohta et al., 2001), we presumed that their target genes might be down-regulated in *Pro-35S:AtERF4-HA* and *Pro-35S:AtERF8-HA* Arabidopsis plants and up-regulated in *aterf4 aterf8* mutants. As described above, the pattern of *ESP/ESR* expression suggested that AtERF4 and AtERF8 targeted *ESP/ESR*. A chromatin immunoprecipitation (ChIP) assay of *Pro-35S:AtERF4-HA* and *Pro-35S:AtERF4-HA* Arabidopsis plants using anti-HA antibody detected the enrichment of the promoter and intron sequences of *ESP/ESR* that contain CCGnC motifs, the target sequence of AtERF4 (Fig. 9; Yang et al., 2009). By contrast, the ChIP assay detected no enrichment of the *ESP/ESR* CDS or the *UBIQUITIN10* (*UBQ10*) sequence (Fig. 9). In addition, the ChIP assay using *Pro-35S:NLS-GFP-HA* Arabidopsis plants did not detect enrichment of the *ESP/ESR* sequences (Fig. 9). These results suggested specific binding of AtERF4 and AtERF8 to *ESP/ESR* in plant cells.

Induction of *AtERF4* and *AtERF8* Expression during Leaf Senescence

We investigated the transcriptional regulation of *AtERF4* and *AtERF8* in leaf senescence. Because the *TEOSINTE BRANCHED1/CYCLOIDEA/PROLIFERATING CELL NUCLEAR ANTIGEN BINDING FACTOR* (*TCP*) genes are reportedly involved in the progression of leaf senescence (Schommer et al., 2008), we confirmed that compared with the wild type, a *tcp3 tcp4 tcp5 tcp10 tcp13* (quintuple *tcp*) mutant displayed delayed yellowing of leaves, decline in chlorophyll content, and *SAG12* activation (Koyama et al., 2010;

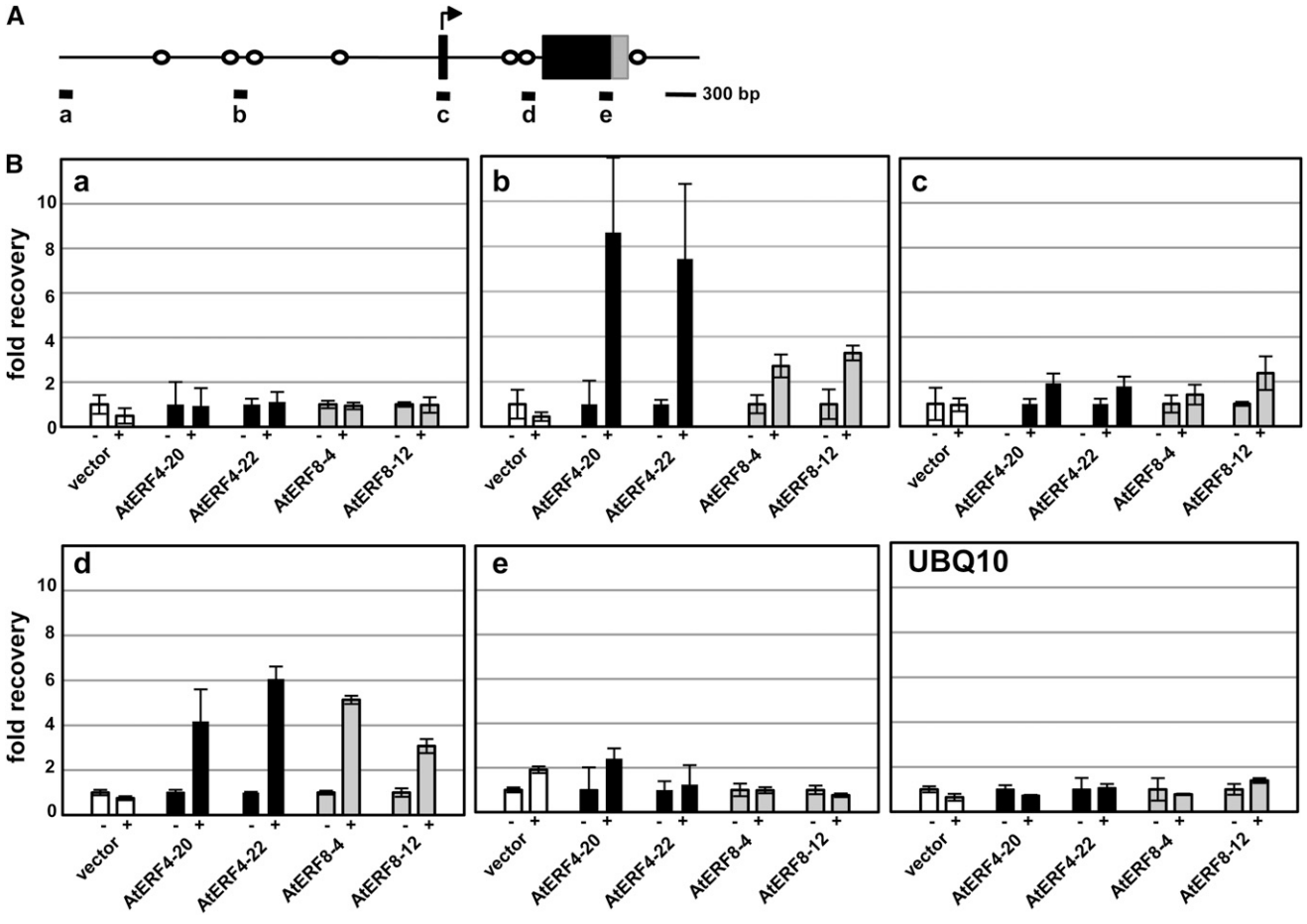

Figure 9. Binding of AtERF4 and AtERF8 to the genomic region of *ESP/ESR*. A, A diagram of the genomic region of *ESP/ESR*. Black and gray boxes indicate the coding and untranslated regions, respectively. White circles show the position of the CCGnC motif, a target sequence of AtERF4. Thick bars below the diagram indicate the regions amplified with sets of primers in the ChIP analysis in B. B, Enrichment of the *ESP/ESR* sequences in the ChIP analysis. Chromatins were prepared from *Pro-35S:NLS-GFP-HA* (vector) and two independent lines of *Pro-35S:AtERF4-HA* (*AtERF4*) and *Pro-35S:AtERF8-HA* (*AtERF8*) Arabidopsis plants, immunoprecipitated in the absence (–) and presence (+) of antibodies, and subjected to quantitative PCR. The fold recovery was relative to the value processed in the absence of antibodies. Error bars indicate SD of technical triplicates.

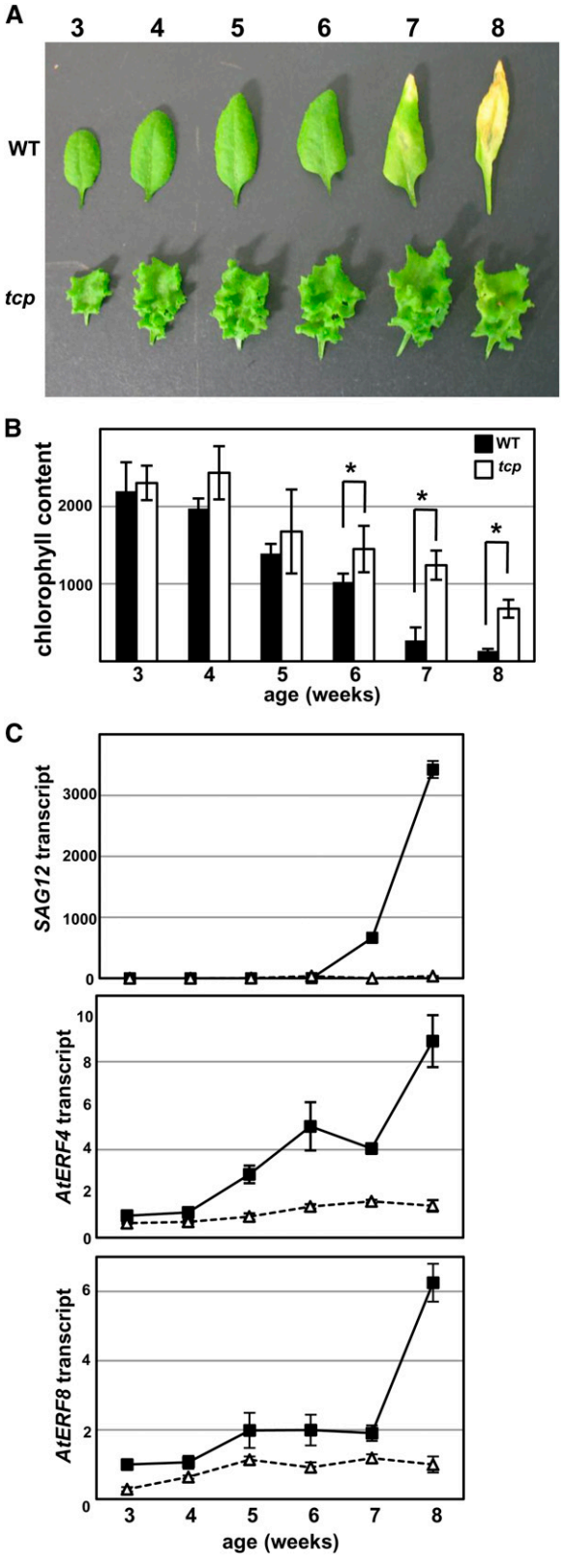

Figure 10. Expression of *AtERF4* and *AtERF8* during leaf senescence of wild-type (WT) and quintuple *tcp* plants. A, The delayed yellowing of leaves in quintuple *tcp* mutant. The sixth leaf of wild-type (top) and quintuple *tcp* (bottom) plants of different ages was photographed. B, Chlorophyll content in the sixth leaf of the wild type and quintuple *tcp* mutant at indicated ages. The error bars and asterisks indicate SD (n = 12) and SDs at $P < 0.001$ by Student's t test. C, Expression of *SAG12*, *AtERF4*, and *AtERF8* in the wild type and the quintuple *tcp* mutant. Transcript levels were determined with RT-PCR using aliquots of total RNAs from the sixth leaves of the wild type (black squares) and quintuple *tcp* mutants (white triangles) at the indicated ages. Each value of 3-week-old leaves was set at 1. Error bars indicate SD of technical triplicates.

Fig. 10, A–C), and we used the quintuple *tcp* mutant as a control for plants with delayed senescence. Our RT-PCR analysis detected basal levels of *AtERF4* and *AtERF8* transcripts in leaves of 3-old-week wild-type plants (Figs. 7B and 10C; Yang et al., 2005). The increase in *AtERF4* and *AtERF8* transcripts began 5 weeks after germination and preceded leaf yellowing, but this increase was delayed in the quintuple *tcp* mutant (Fig. 10C). These results suggested that *AtERF4* and *AtERF8* expression was induced during leaf senescence.

DISCUSSION

Class II ERF Regulatory Cascade for the Progression of Leaf Senescence

The involvement of class II ERFs in the responses to pathogens, salt, ethylene, JA, and ABA has been reported previously (McGrath et al., 2005; Nasir et al., 2005; Song et al., 2005; Yang et al., 2005; Li et al., 2011). In particular, *NbCD1*, a *Nicotiana benthamiana* class II *ERF*, positively regulates cell death in the defense response of tobacco and Arabidopsis (Nasir et al., 2005). Herein, we expand these findings on the proteasome-mediated control of class II ERFs and describe a novel gene regulatory cascade involving AtERF4 and AtERF8 that progresses leaf senescence.

Figure 11A presents our working model of a regulatory cascade involving the class II ERFs that progresses leaf senescence. Our gene expression and ChIP analyses suggest *ESP/ESR* as a direct target of AtERF4 and AtERF8. The ectopic expression of *AtERF4* and *AtERF8* transcriptionally repressed *ESP/ESR*, whereas loss of function of these *ERF* genes derepressed its expression. The inhibitory effect of ESP/ESR on the progression of leaf senescence depends largely on the activity of WRKY53, a positive regulator of leaf senescence (Miao and Zentgraf, 2007). ESP/ESR inhibits the activity of WRKY53 through physical interaction that may prevent WRKY53 DNA-binding activity and then retards leaf senescence. In addition, ESP/ESR transcriptionally suppresses *WRKY53* expression. Because the primary biochemical function of AtERF4 and AtERF8 is the repression of transcription, the repression of *ESP/ESR* by AtERF4 and AtERF8 may activate WRKY53 and, as a consequent, initiate the progression of leaf senescence. The JA-inducible and ecotype-

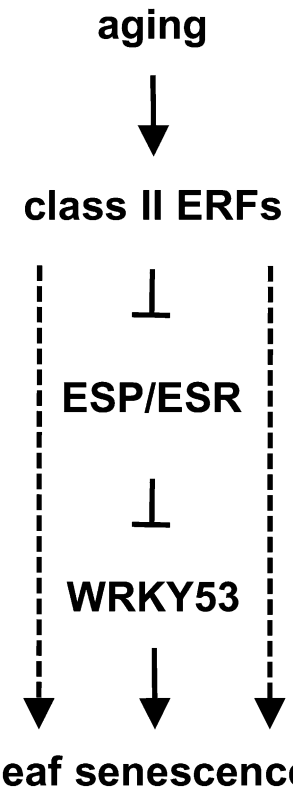

Figure 11. Model showing the roles of the class II ERFs in the progression of leaf senescence. Schematic representation of a regulatory cascade involving the class II ERFs for the progression of leaf senescence. Aging activates AtERF4 and AtERF8 at both the transcriptional and the posttranslational levels. These ERFs directly repress transcription of *ESP/ESR* to derepress the activity of WRKY53. WRKY53 and uncharacterized factors downstream of ERFs are involved in the progression of leaf senescence, as indicated by solid and dashed arrows, respectively.

dependent expression of *ESP/ESR* has been reported (Lambrix et al., 2001; Miao et al., 2007), but the molecular mechanisms of the regulation are unclear. Our findings of the gradual reduction of *ESP/ESR* expression during aging (Supplemental Fig. S5) and its regulation by class II ERFs provide novel insights into the regulation of *ESP/ESR*.

The ectopic expression of *AtERF4* and *AtERF8* induced expression of *WRKY30*, *WRKY53*, and *WRKY75* genes, which positively regulated leaf senescence, whereas loss of function of these *ERF* genes inhibited their expression. By contrast, AtERF4 did not change the expression of *WRKY6*, another regulator of the progression of leaf senescence, in our microarray analysis (Supplemental Table S3). These results suggest that the expression of *WRKY30*, *WRKY53*, and *WRKY75* genes are positively regulated by AtERF4 and AtERF8 but not the general effects of the leaf senescence-associated phenotype. In addition to aging and *ESP/ESR*, salicylate, H_2O_2, pathogens, a mitogen-activated protein kinase kinase kinase, and histone methylation are involved in the regulation of *WRKY53* (Miao et al., 2007; Miao and Zentgraf, 2007; Ay et al., 2009). Interaction between WRKY30 and WRKY53 in yeast (*Saccharomyces cerevisiae*) two-hybrid system suggests the possible involvement of these WRKYs in the same signaling pathway (Besseau et al., 2012). By contrast, the regulation of *WRKY30* and *WRKY75* is almost unknown. Our results characterize *AtERF4* and *AtERF8* as novel regulators of these *WRKY* genes. Involvement of ESP/ESR and WRKY53 in the regulation of expression of *WRKY30* and *WRKY75* remains unclear.

Moreover, AtERF4 and AtERF8 might regulate these *WRKY* genes directly and indirectly in uncharacterized pathways. In addition to *ESP/ESR*, AtERF4 and AtERF8 negatively regulate the expression of many genes, including *AUX/IAA* genes. Several studies have reported on both the positive and the negative roles of auxin in the progression of leaf senescence (Ellis et al., 2005; van der Graaff et al., 2006; Hou et al., 2013). Because IAA3/SHY2 suppresses expression of auxin-inducible genes through physical interactions with AUXIN RESPONSE FACTORs (ARFs) and several ARFs act as positive regulators of leaf senescence (Ellis et al., 2005; Weijers et al., 2005), the negative effects on IAA3/SHY2 by AtERF4 and AtERF8 may be involved in the progression of leaf senescence. The repression of *AUX/IAA* transcriptions by AtERF4 and AtERF8 may be responsible for a specific, rather than a general, role of auxin in the progression of leaf senescence.

Because plants stimulate leaf senescence prematurely under unfavorable conditions (Buchanan-Wollaston et al., 2003; Lim et al., 2007), stress responsive genes downstream of AtERF4 and AtERF8 likely contribute to signaling pathway integration for the regulation of leaf senescence. *ESP/ESR*, the target of AtERF4 and AtERF8, has important roles in defense against herbivores and pathogens (Lambrix et al., 2001; Miao et al., 2007). *WRKY* genes are involved in leaf senescence and various stress responses (Rushton et al., 2010). *WRKY53* and *WRKY75* are involved in responses to biotic stress and nutrient starvation, respectively (Devaiah et al., 2007; Miao and Zentgraf, 2007). *WRKY18*, *WRKY40*, and *WRKY60* enhance the basal defense system against pathogens (Xu et al., 2006). In addition, our microarray analysis suggested that AtERF4 up-regulates *ORE1*, *ERF1*, *JASMONATE ZIM-DOMAIN1*, *ZINC FINGER OF ARABIDOPSIS THALIANA7* (*ZAT7*), *ZAT10*, *ZAT12*, *MYB2*, and *MYB44*, which regulate responses to ethylene, JA, ABA, H_2O_2, and dehydration (Solano et al., 1998; Sakamoto et al., 2004; Davletova et al., 2005; Chini et al., 2007; Ciftci-Yilmaz et al., 2007; Thines et al., 2007; Jung et al., 2008; Kim et al., 2009; Guo and Gan, 2011). Because these stresses affect the progression of leaf senescence, we postulate that these class II ERFs may integrate aging and stress signaling pathways. Whereas the similar phenotype of *Pro-35S:NLS-GFP-NtERF3* Arabidopsis plants to those of *Pro-35S:AtERF4-HA* and *Pro-35S:AtERF8-HA* Arabidopsis plants suggests the involvement of NtERF3 in the progression of cell death and leaf senescence, the downstream genes of NtERF3 in tobacco plants remain to be clarified.

Proteolytic Control of Class II ERFs by Proteasomes

We demonstrate that aging stimulates expression of *AtERF4* and *AtERF8* in leaves and increases ERF accumulation. In addition to elucidating the stress response-associated transcriptional control of class II *ERF*s (Suzuki et al., 1998; Yamamoto et al., 1999; Fujimoto et al., 2000; Kitajima et al., 2000; Nishiuchi et al., 2004), our study adds some insights to the developmental regulation of these ERFs. The induction of *AtERF4* and *AtERF8* expression through aging is consistent with data from several transcriptome analyses (Breeze et al., 2011), suggesting robust developmental control of *AtERF4* and *AtERF8* during leaf senescence. The delayed induction of *AtERF4* and *AtERF8* expression in quintuple *tcp* mutant leaves suggests the involvement of the *TCP* genes in the regulation of class II ERFs, although the detailed mechanisms of this induction remain unclear. The progression of leaf senescence requires the coordination of many signals, and the regulation of class II ERFs during senescence is considered to be under the control of a complex process.

Because the class II ERFs act as positive regulators of leaf senescence, our results suggest that both transcriptional activation and posttranslational stabilization of AtERF4 and AtERF8 are important for the progression of senescence. The fine-tuning of their accumulation may set the pace of the progression of leaf senescence. In younger plants, proteolytic regulation maintains low levels of class II ERFs (Fig. 3). The severe cell death observed in the transgenic Arabidopsis plants with constitutive accumulation of NtERF3 (Δ83/190) demonstrates that the enhanced and continuous accumulation of class II ERFs causes premature death. *AtERF4* and *AtERF8* transcripts are maintained at basal levels in younger leaves (Figs. 7B and 10C; Yang et al., 2005), but rapidly activated to cope with various environmental stimuli (McGrath et al., 2005; Nasir et al., 2005; Song et al., 2005; Yang et al., 2005). Therefore, proteolytic regulation may prevent their excess and prolonged accumulation to protect cells against premature death.

Whereas selective protein turnover is regulated by proteasomes during leaf senescence, bulk protein degradation is processed by autophagy (Vierstra, 2009). Prior studies have described the role of several components of the ubiquitin-proteasome system (Woo et al., 2001; Gepstein, 2004; Lin and Wu, 2004; Buchanan-Wollaston et al., 2005; van der Graaff et al., 2006; Peng et al., 2007; Raab et al., 2009; Miao and Zentgraf, 2010; Breeze et al., 2011). In particular, WRKY53 is degraded by a homologous to the E6-AP carboxyl terminus domain ubiquitin ligase (Miao and Zentgraf, 2010). Our present study suggests that proteolytic control of class II ERFs by proteasomes occurs and these factors are involved in the progression of leaf senescence. In addition to the characterization of NtUBC2 as an interaction partner of NtERF3 (Koyama et al., 2003), investigations for identification of components that degrade class II ERFs remain to be performed. These class II ERFs interact with the corepressor TOPLESS to negatively regulate target gene transcription (Causier et al., 2012). The posttranslational control of class II ERFs by proteasomes suggests that a sophisticated mechanism may underlie the progression of leaf senescence.

In summary, we showed the proteasomal regulation, age-dependent accumulation, and regulatory cascade of class II ERFs during leaf development. Our results provide cues of a sophisticated mechanism for the progression of leaf senescence involving class II ERFs.

MATERIALS AND METHODS

Plant Materials and Growth Conditions

Growth conditions and the transformation of tobacco (*Nicotiana tabacum*) XD6S cells and Arabidopsis (*Arabidopsis thaliana*) plants have been described previously (Yamamoto et al., 1999; Koyama et al., 2010). Arabidopsis ecotype Columbia was used throughout this study unless otherwise indicated. *erf4-1* (SALK_073394; Alonso et al., 2003; McGrath et al., 2005) and *erf8-1* (FLAG157D10; Wassilewskija; Samson et al., 2002) were crossed three times to Columbia plants before use. The *tcp* quintuple mutant (*tcp3 tcp4 tcp5 tcp10 tcp13*) has been described previously (Koyama et al., 2010).

Plasmids

For recombinant protein production in *Escherichia coli*, the CDSs of *NtERF2*, *NtERF3*, *GFP*, and various regions of *NtERF3* were cloned into pET32 (Novagen). For the expression of *GFP* fusion genes in plant cells, the *NLS* of the SV-40 T antigen from pGAD424 (Clontech) was inserted upstream of *GFP*, and the entire or partial CDSs of *NtERF3* were cloned downstream of *GFP*. The resulting fusion *GFP* genes were individually inserted into pBI101 for the transformation of tobacco XD6S cells and Arabidopsis plants. For the overexpression of *AtERF4* and *AtERF8*, the CDSs without the stop codon of *AtERF4* and *AtERF8* were respectively ligated into p35SHAG, in which the LDLDLELRLGFA sequence of p35SSRDXG was replaced by the *HA* sequence and transferred into pBCKH (Mitsuda et al., 2006). The primers used for plasmid construction are listed in Supplemental Table S5.

In Vitro Degradation Assay

The 6× His-tagged NtERFs and GFP were produced in *E. coli*, purified using a nickel-chelating resin according to manufacturer instructions (Amersham Pharmacia), and dialyzed against a solution containing 20 mM Tris (pH 8.0) and 100 mM NaCl. The cell-free degradation assay was modified from previous reports as described below (Osterlund et al., 2000). For preparation of the extract solution, cultured tobacco XD6S cells were ground in liquid nitrogen, suspended in a buffer containing 50 mM Tris (pH 7.5), 10 mM NaCl, 10 mM $MgCl_2$, 5 mM dithiothreitol, 2 mM ATP, and COMPLETE EDTA-free Protease Inhibitor Cocktail (Promega), and centrifuged at 15,000 rpm for 10 min at 4°C. The supernatant was diluted to 4 mg mL^{-1} to make the cell extract solution. Aliquots containing 100 ng recombinant NtERFs and GFP were added into 200 μL cell extract solution, incubated at room temperature for 0, 15, 30, or 60 min, mixed in an equal volume of 2× SDS loading buffer (Tris, pH 6.8, 2% SDS (w/v), 1 mM EDTA, and 2-mercaptoethanol), and boiled to terminate the reaction. The proteins were separated by SDS-PAGE, blotted onto Immobilon-P membranes (Millipore), and subjected to immunoblot analysis.

Preparation of Tobacco and Arabidopsis Proteins

For preparation of plant protein samples, tobacco XD6S callus lines at 2 weeks after the inoculation on new plates and Arabidopsis seedlings grown on Murashige and Skoog plates were ground in liquid nitrogen, suspended in extraction buffer (Tris, pH 6.8, 8 M urea, 0.5% SDS (w/v), 1 mM EDTA, and 2-mercaptoethanol), incubated for 2 min at 95°C, and mixed with one-third volume of SDS/urea loading buffer (Tris, pH 6.8, 8 M urea, 0.5% SDS (w/v), 1 mM EDTA, and 2-mercaptoethanol). Aliquots containing 10 and 30 μg of protein from tobacco XD6S cells and Arabidopsis plants, respectively, were

separated using SDS-PAGE, blotted onto Immobilon-P membranes, and subjected to immunoblot analysis.

Antibodies and Immunoblot Analysis

For production of anti-NtERF2 and anti-NtERF3 antibodies, the recombinant NtERF2 and NtERF3 proteins fused with maltose-binding protein were produced in *E. coli*, purified using an amylose resin (New England Laboratory) according to manufacturer instructions, and injected into rabbits. For immunoblot analysis, membranes were incubated with the appropriate primary and secondary antibodies. The antibodies used were as follows: anti-NtERF2 and anti-NtERF3 antibodies (1:2,000), anti-GFP antibody (1:5,000; Medical and Biological Laboratory), peroxidase-conjugated anti-HA antibody (1:500; Roche), and peroxidase-conjugated anti-rabbit IgG (1:10,000; Medical and Biological Laboratory). Immunoreactive proteins were detected using the ECL Plus Western Blotting Kit (GE Healthcare).

Microscopy

The fluorescence images in Figure 2, A and C were, respectively, monitored with an Olympus BHS-RFC as described previously (Ohta et al., 2000) and a Keyence BZ-9000 with a GFP Bandpass filter at a fixed one-third second exposure. Bright field images were obtained with a Leica MZ FL III.

Gene Expression Analysis

Total RNA was prepared from tobacco XD6S cells and Arabidopsis plants using TRIzol reagent, FastRNA Green (Qbiogene), or RNeasy Plant Mini (Qiagen) kits. RNA blot analysis was performed as described previously (Koyama et al., 2003). For RT, templates were reverse transcribed from total RNA using SuperScript II first-strand complementary DNA synthesis (Invitrogen). Real-time PCR was performed using first-strand complementary DNA, a pair of primers (Supplemental Table S5), and iQTM CYBR Green PCR Supermix (Bio-Rad) with a CFX96 real-time PCR system (Bio-Rad). Transcript levels were detected in triplicate using a standard curve derived from the reference sample. The relative values of the transcripts were normalized to the *UBQ1* level.

Microarray analysis was performed with the two-color method using aliquots of total RNA from four biological replicates of 2-week-old *Pro-35S:AtERF4-HA* (line no. 20) and *Pro-35S:NLS-GFP-HA* Arabidopsis plants with an Agilent Arabidopsis V3 (4x44k) microarray. We used previously described preparation and statistical analyses (Koyama et al., 2010) with the following exceptions. Only genes with average detection values of at least 1.5 in both test and reference samples were analyzed. The *P* value for each gene was calculated using a dependent Student's *t* test. To estimate the FDR, we calculated the *Q* value from the *P* value using QVALUE software with the default settings (Storey and Tibshirani, 2003) and selected up- and down-regulated (>2-fold and <0.5-fold) genes with a *P* value of 0.05 or less (FDR < 0.04225). In Figure 5, the transcript level of each gene at different ages was calculated as relative to that at 19 d after sowing (Breeze et al., 2011), and a clustered heat map was prepared using Cluster3 software (Eisen et al., 1998). To evaluate overrepresentation of some gene lists among up- and down-regulated genes, we performed a binomial test using R (http://www.r-project.org/).

ChIP

Nuclear extract was prepared from 3-week-old Arabidopsis plants, subjected to sonication, and immunoprecipitated with 500 ng anti-HA antibody (clone 3F10; Roche) as described previously (Koyama et al., 2010). The chromatin precipitated was reverse cross linked and purified with ethanol and served as a template for PCR (CFX96 real-time PCR system; Bio-Rad) using an appropriate set of primers (Supplemental Table S5). The values were calculated with a standard curve generated from the input sample and normalized using a background value determined from the eukaryotic INITIATION FACTOR4A sequence. Figure 10 shows a representative from three biological replicates with similar trends.

Chemical Treatment of Plants

For MG132 treatment, Arabidopsis plants were immersed in a solution containing 50 mM MES (pH 5.7), 0.05% (v/v) Tween 20, and 50 μM MG132 (Calbiochem) for 6 h in light. For trypan blue staining, Arabidopsis plants were immersed in trypan blue solution (25% (v/v) lactic acid, 23% (v/v) phenol, and 2.5 mg mL^{-1} trypan blue [Sigma]) for 1 h and rinsed several times in chloral hydrate solution (25 g chloral hydrate in 10 mL water). For DAB staining, Arabidopsis plants were incubated in DAB buffer (50 mM Tris-acetate, pH 5.0, 0.05% (v/v) Tween 20, 1 mg mL^{-1} DAB [Serva]) in the dark for 24 h, cleared in boiling ethanol, and rendered transparent in chloral hydrate solution.

Dark-Induced Senescence Assay

The sixth leaves were detached from 5-week-old Arabidopsis plants, floated on water, and incubated in the dark. For chlorophyll extraction, the leaves were soaked in 80% (v/v) acetone. The chlorophyll content was determined via spectrophotometric analysis (Lichtenthaler and Buschmann, 2001) and normalized to the fresh weight of the leaves.

Sequence data from this article can be found in the GenBank or Arabidopsis Genome Initiative data libraries under accession numbers NtERF3 (D38124), AtERF4 (AT3G15210), AtERF8 (AT1G53170), WRKY18 (AT4G31800), WRKY30 (AT5G24110), WRKY40 (AT1G80840), WRKY53 (AT4G23810), WRKY60 (AT2G25000), WRKY75 (AT5G13080), ESP/ESR (AT1G54040), IAA3/SHY2 (AT1G04240), IAA6/SHY1 (AT1G52830), IAA29 (AT4G32280), SAG12 (AT5G45890), SAG13 (AT2G29350), UBQ1 (AT3G52590), UBQ10 (AT4G05320), and eukaryotic INITIATION FACTOR4A (AT3G13920). Microarray data from this article can be found in the National Center for Biotechnology Information Gene Expression Omnibus (http://www.ncbi.nlm.nih.gov/geo/) under accession number GSE41053.

Supplemental Data

The following materials are available in the online version of this article.

Supplemental Figure S1. Production and purification of NtERF proteins in *E. coli*.

Supplemental Figure S2. Expression of *NtERF3*, *AtERF4*, *AtERF8*, and *GFP* genes in tobacco XD6S callus lines and Arabidopsis plants.

Supplemental Figure S3. Expression of *SAG* genes in *Pro-35S:AtERF4-HA* Arabidopsis plants.

Supplemental Figure S4. Leaf senescence of *aterf4* and *aterf8* single mutants.

Supplemental Figure S5. Expression of *ESP/ESR* during leaf senescence in wild-type leaves.

Supplemental Figure S6. Timing of flowering in wild-type and *aterf4 aterf8* double mutant plants.

Supplemental Figure S7. An ethylene precursor- and methyl jasmonate-stimulated dark-induced senescence of *aterf4 aterf8* double mutant leaves.

Supplemental Table S1. Cis-elements enriched in the genes regulated in *35S:AtERF4-HA* plants.

Supplemental Table S2. Families containing the genes up- and down-regulated in *35S:AtERF4-HA* plants.

Supplemental Table S3. Expression of *WRKY* genes in *35S:AtERF4-HA* plants.

Supplemental Table S4. Expression of *AUX/IAA* genes in *35S:AtERF4-HA* plants.

Supplemental Table S5. Primers used in this study.

ACKNOWLEDGMENTS

We thank the Arabidopsis Biological Resource Center and the French National Institute of Agricultural Research for providing seeds, Yuko Takiguchi for her technical contribution regarding the microarray experiment, and Ryouhei Terauchi, Hiroyuki Kanzaki, Hideaki Shinshi, Kaoru Suzuki, Keiichiro Hiratsu, and Kyoko Matsui for helpful discussions.

Received March 19, 2013; accepted April 25, 2013; published April 29, 2013.

LITERATURE CITED

Alonso JM, Stepanova AN, Leisse TJ, Kim CJ, Chen H, Shinn P, Stevenson DK, Zimmerman J, Barajas P, Cheuk R, et al (2003) Genome-wide insertional mutagenesis of *Arabidopsis thaliana*. Science **301:** 653–657

Asher G, Reuven N, Shaul Y (2006) 20S proteasomes and protein degradation "by default." Bioessays **28:** 844–849

Ay N, Irmler K, Fischer A, Uhlemann R, Reuter G, Humbeck K (2009) Epigenetic programming via histone methylation at WRKY53 controls leaf senescence in *Arabidopsis thaliana*. Plant J **58:** 333–346

Balazadeh S, Riaño-Pachón DM, Mueller-Roeber B (2008) Transcription factors regulating leaf senescence in *Arabidopsis thaliana*. Plant Biol (Stuttg) **10:** 63–75

Balazadeh S, Kwasniewski M, Caldana C, Mehrnia M, Zanor MI, Xue GP, Mueller-Roeber B (2011) ORS1, an H_2O_2-responsive NAC transcription factor, controls senescence in *Arabidopsis thaliana*. Mol Plant **4:** 346–360

Besseau S, Li J, Palva ET (2012) WRKY54 and WRKY70 co-operate as negative regulators of leaf senescence in *Arabidopsis thaliana*. J Exp Bot **63:** 2667–2679

Breeze E, Harrison E, McHattie S, Hughes L, Hickman R, Hill C, Kiddle S, Kim YS, Penfold CA, Jenkins D, et al (2011) High-resolution temporal profiling of transcripts during *Arabidopsis* leaf senescence reveals a distinct chronology of processes and regulation. Plant Cell **23:** 873–894

Buchanan-Wollaston V, Earl S, Harrison E, Mathas E, Navabpour S, Page T, Pink D (2003) The molecular analysis of leaf senescence—a genomics approach. Plant Biotechnol J **1:** 3–22

Buchanan-Wollaston V, Page T, Harrison E, Breeze E, Lim PO, Nam HG, Lin JF, Wu SH, Swidzinski J, Ishizaki K, et al (2005) Comparative transcriptome analysis reveals significant differences in gene expression and signalling pathways between developmental and dark/starvation-induced senescence in Arabidopsis. Plant J **42:** 567–585

Causier B, Ashworth M, Guo W, Davies B (2012) The TOPLESS interactome: a framework for gene repression in Arabidopsis. Plant Physiol **158:** 423–438

Chini A, Fonseca S, Fernández G, Adie B, Chico JM, Lorenzo O, García-Casado G, López-Vidriero I, Lozano FM, Ponce MR, et al (2007) The JAZ family of repressors is the missing link in jasmonate signalling. Nature **448:** 666–671

Ciftci-Yilmaz S, Morsy MR, Song L, Coutu A, Krizek BA, Lewis MW, Warren D, Cushman J, Connolly EL, Mittler R (2007) The EAR-motif of the Cys2/His2-type zinc finger protein Zat7 plays a key role in the defense response of Arabidopsis to salinity stress. J Biol Chem **282:** 9260–9268

Davletova S, Schlauch K, Coutu J, Mittler R (2005) The zinc-finger protein Zat12 plays a central role in reactive oxygen and abiotic stress signaling in Arabidopsis. Plant Physiol **139:** 847–856

Devaiah BN, Karthikeyan AS, Raghothama KG (2007) WRKY75 transcription factor is a modulator of phosphate acquisition and root development in Arabidopsis. Plant Physiol **143:** 1789–1801

Dreher K, Callis J (2007) Ubiquitin, hormones and biotic stress in plants. Ann Bot (Lond) **99:** 787–822

Eisen MB, Spellman PT, Brown PO, Botstein D (1998) Cluster analysis and display of genome-wide expression patterns. Proc Natl Acad Sci USA **95:** 14863–14868

Ellis CM, Nagpal P, Young JC, Hagen G, Guilfoyle TJ, Reed JW (2005) AUXIN RESPONSE FACTOR1 and AUXIN RESPONSE FACTOR2 regulate senescence and floral organ abscission in *Arabidopsis thaliana*. Development **132:** 4563–4574

Fujimoto SY, Ohta M, Usui A, Shinshi H, Ohme-Takagi M (2000) *Arabidopsis* ethylene-responsive element binding factors act as transcriptional activators or repressors of GCC box-mediated gene expression. Plant Cell **12:** 393–404

Gan S, Amasino RM (1997) Making sense of senescence (molecular genetic regulation and manipulation of leaf senescence). Plant Physiol **113:** 313–319

Gepstein S (2004) Leaf senescence—not just a 'wear and tear' phenomenon. Genome Biol **5:** 212

Guo Y, Gan S (2006) AtNAP, a NAC family transcription factor, has an important role in leaf senescence. Plant J **46:** 601–612

Guo Y, Gan S (2011) AtMYB2 regulates whole plant senescence by inhibiting cytokinin-mediated branching at late stages of development in Arabidopsis. Plant Physiol **156:** 1612–1619

Hou K, Wu W, Gan SS (2013) *SAUR36*, a small auxin up RNA gene, is involved in the promotion of leaf senescence in Arabidopsis. Plant Physiol **161:** 1002–1009

Jung C, Seo JS, Han SW, Koo YJ, Kim CH, Song SI, Nahm BH, Choi YD, Cheong JJ (2008) Overexpression of AtMYB44 enhances stomatal closure to confer abiotic stress tolerance in transgenic Arabidopsis. Plant Physiol **146:** 623–635

Kim JH, Woo HR, Kim J, Lim PO, Lee IC, Choi SH, Hwang D, Nam HG (2009) Trifurcate feed-forward regulation of age-dependent cell death involving miR164 in Arabidopsis. Science **323:** 1053–1057

Kitajima S, Koyama T, Ohme-Takagi M, Shinshi H, Sato F (2000) Characterization of gene expression of NsERFs, transcription factors of basic PR genes from *Nicotiana sylvestris*. Plant Cell Physiol **41:** 817–824

Koyama T, Mitsuda N, Seki M, Shinozaki K, Ohme-Takagi M (2010) TCP transcription factors regulate the activities of ASYMMETRIC LEAVES1 and miR164, as well as the auxin response, during differentiation of leaves in *Arabidopsis*. Plant Cell **22:** 3574–3588

Koyama T, Okada T, Kitajima S, Ohme-Takagi M, Shinshi H, Sato F (2003) Isolation of tobacco ubiquitin-conjugating enzyme cDNA in a yeast two-hybrid system with tobacco ERF3 as bait and its characterization of specific interaction. J Exp Bot **54:** 1175–1181

Lambrix V, Reichelt M, Mitchell-Olds T, Kliebenstein DJ, Gershenzon J (2001) The *Arabidopsis* epithiospecifier protein promotes the hydrolysis of glucosinolates to nitriles and influences *Trichoplusia ni* herbivory. Plant Cell **13:** 2793–2807

Lee S, Seo PJ, Lee HJ, Park CM (2012) A NAC transcription factor NTL4 promotes reactive oxygen species production during drought-induced leaf senescence in Arabidopsis. Plant J **70:** 831–844

Li Z, Zhang L, Yu Y, Quan R, Zhang Z, Zhang H, Huang R (2011) The ethylene response factor AtERF11 that is transcriptionally modulated by the bZIP transcription factor HY5 is a crucial repressor for ethylene biosynthesis in Arabidopsis. Plant J **68:** 88–99

Li Z, Peng J, Wen X, Guo H (2012) Gene network analysis and functional studies of senescence-associated genes reveal novel regulators of Arabidopsis leaf senescence. J Integr Plant Biol **54:** 526–539

Lichtenthaler HK, Buschmann C (2001) Chlorophylls and carotenoids: measurement and characterization by UV-VIS spectroscopy. *In* **Wrolstad RE, Acree TE, An H, Decker EA, Penner MH, Reid DS, Schwartz SJ, Shoemaker CF, Sporns P**, eds, Current Protocols in Food Analytical Chemistry. Wiley & Sons, New York

Lim PO, Kim HJ, Nam HG (2007) Leaf senescence. Annu Rev Plant Biol **58:** 115–136

Lin JF, Wu SH (2004) Molecular events in senescing Arabidopsis leaves. Plant J **39:** 612–628

McGrath KC, Dombrecht B, Manners JM, Schenk PM, Edgar CI, Maclean DJ, Scheible WR, Udvardi MK, Kazan K (2005) Repressor- and activator-type ethylene response factors functioning in jasmonate signaling and disease resistance identified via a genome-wide screen of Arabidopsis transcription factor gene expression. Plant Physiol **139:** 949–959

Miao Y, Laun T, Zimmermann P, Zentgraf U (2004) Targets of the WRKY53 transcription factor and its role during leaf senescence in Arabidopsis. Plant Mol Biol **55:** 853–867

Miao Y, Laun TM, Smykowski A, Zentgraf U (2007) Arabidopsis MEKK1 can take a short cut: it can directly interact with senescence-related WRKY53 transcription factor on the protein level and can bind to its promoter. Plant Mol Biol **65:** 63–76

Miao Y, Zentgraf U (2007) The antagonist function of *Arabidopsis* WRKY53 and ESR/ESP in leaf senescence is modulated by the jasmonic and salicylic acid equilibrium. Plant Cell **19:** 819–830

Miao Y, Zentgraf U (2010) A HECT E3 ubiquitin ligase negatively regulates Arabidopsis leaf senescence through degradation of the transcription factor WRKY53. Plant J **63:** 179–188

Mitsuda N, Hiratsu K, Todaka D, Nakashima K, Yamaguchi-Shinozaki K, Ohme-Takagi M (2006) Efficient production of male and female sterile plants by expression of a chimeric repressor in Arabidopsis and rice. Plant Biotechnol J **4:** 325–332

Mizoi J, Shinozaki K, Yamaguchi-Shinozaki K (2012) AP2/ERF family transcription factors in plant abiotic stress responses. Biochim Biophys Acta **1819:** 86–96

Nakano T, Suzuki K, Fujimura T, Shinshi H (2006) Genome-wide analysis of the ERF gene family in Arabidopsis and rice. Plant Physiol **140:** 411–432

Nasir KH, Takahashi Y, Ito A, Saitoh H, Matsumura H, Kanzaki H, Shimizu T, Ito M, Fujisawa S, Sharma PC, et al (2005) High-throughput in planta expression screening identifies a class II ethylene-responsive element binding factor-like protein that regulates plant cell death and non-host resistance. Plant J **43:** 491–505

Nishiuchi T, Shinshi H, Suzuki K (2004) Rapid and transient activation of transcription of the ERF3 gene by wounding in tobacco leaves: possible involvement of NtWRKYs and autorepression. J Biol Chem **279:** 55355–55361

Oh SA, Park JH, Lee GI, Paek KH, Park SK, Nam HG (1997) Identification of three genetic loci controlling leaf senescence in *Arabidopsis thaliana*. Plant J **12:** 527–535

Ohta M, Matsui K, Hiratsu K, Shinshi H, Ohme-Takagi M (2001) Repression domains of class II ERF transcriptional repressors share an essential motif for active repression. Plant Cell **13:** 1959–1968

Ohta M, Ohme-Takagi M, Shinshi H (2000) Three ethylene-responsive transcription factors in tobacco with distinct transactivation functions. Plant J **22:** 29–38

Osterlund MT, Hardtke CS, Wei N, Deng XW (2000) Targeted destabilization of HY5 during light-regulated development of Arabidopsis. Nature **405:** 462–466

Peng M, Hannam C, Gu H, Bi YM, Rothstein SJ (2007) A mutation in NLA, which encodes a RING-type ubiquitin ligase, disrupts the adaptability of Arabidopsis to nitrogen limitation. Plant J **50:** 320–337

Raab S, Drechsel G, Zarepour M, Hartung W, Koshiba T, Bittner F, Hoth S (2009) Identification of a novel E3 ubiquitin ligase that is required for suppression of premature senescence in Arabidopsis. Plant J **59:** 39–51

Robatzek S, Somssich IE (2002) Targets of AtWRKY6 regulation during plant senescence and pathogen defense. Genes Dev **16:** 1139–1149

Rushton PJ, Somssich IE, Ringler P, Shen QJ (2010) WRKY transcription factors. Trends Plant Sci **15:** 247–258

Sakamoto H, Maruyama K, Sakuma Y, Meshi T, Iwabuchi M, Shinozaki K, Yamaguchi-Shinozaki K (2004) Arabidopsis Cys2/His2-type zinc-finger proteins function as transcription repressors under drought, cold, and high-salinity stress conditions. Plant Physiol **136:** 2734–2746

Samson F, Brunaud V, Balzergue S, Dubreucq B, Lepiniec L, Pelletier G, Caboche M, Lecharny A (2002) FLAGdb/FST: a database of mapped flanking insertion sites (FSTs) of *Arabidopsis thaliana* T-DNA transformants. Nucleic Acids Res **30:** 94–97

Schommer C, Palatnik JF, Aggarwal P, Chételat A, Cubas P, Farmer EE, Nath U, Weigel D (2008) Control of jasmonate biosynthesis and senescence by miR319 targets. PLoS Biol **6:** e230

Sharabi-Schwager M, Lers A, Samach A, Guy CL, Porat R (2010) Overexpression of the CBF2 transcriptional activator in Arabidopsis delays leaf senescence and extends plant longevity. J Exp Bot **61:** 261–273

Solano R, Stepanova A, Chao Q, Ecker JR (1998) Nuclear events in ethylene signaling: a transcriptional cascade mediated by ETHYLENE-INSENSITIVE3 and ETHYLENE-RESPONSE-FACTOR1. Genes Dev **12:** 3703–3714

Song CP, Agarwal M, Ohta M, Guo Y, Halfter U, Wang P, Zhu JK (2005) Role of an *Arabidopsis* AP2/EREBP-type transcriptional repressor in abscisic acid and drought stress responses. Plant Cell **17:** 2384–2396

Storey JD, Tibshirani R (2003) Statistical significance for genomewide studies. Proc Natl Acad Sci USA **100:** 9440–9445

Suzuki K, Suzuki N, Ohme-Takagi M, Shinshi H (1998) Immediate early induction of mRNAs for ethylene-responsive transcription factors in tobacco leaf strips after cutting. Plant J **15:** 657–665

Thines B, Katsir L, Melotto M, Niu Y, Mandaokar A, Liu G, Nomura K, He SY, Howe GA, Browse J (2007) JAZ repressor proteins are targets of the SCF(COI1) complex during jasmonate signalling. Nature **448:** 661–665

van der Graaff E, Schwacke R, Schneider A, Desimone M, Flügge UI, Kunze R (2006) Transcription analysis of Arabidopsis membrane transporters and hormone pathways during developmental and induced leaf senescence. Plant Physiol **141:** 776–792

Vierstra RD (2009) The ubiquitin-26S proteasome system at the nexus of plant biology. Nat Rev Mol Cell Biol **10:** 385–397

Weaver LM, Amasino RM (2001) Senescence is induced in individually darkened Arabidopsis leaves, but inhibited in whole darkened plants. Plant Physiol **127:** 876–886

Weijers D, Benkova E, Jäger KE, Schlereth A, Hamann T, Kientz M, Wilmoth JC, Reed JW, Jürgens G (2005) Developmental specificity of auxin response by pairs of ARF and Aux/IAA transcriptional regulators. EMBO J **24:** 1874–1885

Woo HR, Chung KM, Park JH, Oh SA, Ahn T, Hong SH, Jang SK, Nam HG (2001) ORE9, an F-box protein that regulates leaf senescence in *Arabidopsis*. Plant Cell **13:** 1779–1790

Woo HR, Kim JH, Kim J, Kim J, Lee U, Song IJ, Kim JH, Lee HY, Nam HG, Lim PO (2010) The RAV1 transcription factor positively regulates leaf senescence in Arabidopsis. J Exp Bot **61:** 3947–3957

Wu A, Allu AD, Garapati P, Siddiqui H, Dortay H, Zanor MI, Asensi-Fabado MA, Munné-Bosch S, Antonio C, Tohge T, et al (2012) JUNGBRUNNEN1, a reactive oxygen species-responsive NAC transcription factor, regulates longevity in *Arabidopsis*. Plant Cell **24:** 482–506

Xu X, Chen C, Fan B, Chen Z (2006) Physical and functional interactions between pathogen-induced *Arabidopsis* WRKY18, WRKY40, and WRKY60 transcription factors. Plant Cell **18:** 1310–1326

Yamamoto S, Suzuki K, Shinshi H (1999) Elicitor-responsive, ethylene-independent activation of GCC box-mediated transcription that is regulated by both protein phosphorylation and dephosphorylation in cultured tobacco cells. Plant J **20:** 571–579

Yang Z, Tian L, Latoszek-Green M, Brown D, Wu K (2005) Arabidopsis ERF4 is a transcriptional repressor capable of modulating ethylene and abscisic acid responses. Plant Mol Biol **58:** 585–596

Yang S, Wang S, Liu X, Yu Y, Yue L, Wang X, Hao D (2009) Four divergent Arabidopsis ethylene-responsive element-binding factor domains bind to a target DNA motif with a universal CG step core recognition and different flanking bases preference. FEBS J **276:** 7177–7186